Recombinant human granulocyte colony-stimulating factor alleviates liver fibrosis in bile duct-ligated mice

Huy Quang Do[1], Trinh Van Le[1], Minh Thanh Dang[1,], Tien-Trieu Pham-Le[1], Luan Van Tran[1], Khon Chan Huynh[2], Ai-Xuan Le Holterman[3], Nhung Hai Truong[1,4,*]

[1]Laboratory of Stem Cell Research and Application, University of Science, Vietnam National University, Ho Chi Minh city, Vietnam

[2]Biomedical Engineering Department, International University, Vietnam National University, Ho Chi Minh city, Vietnam

[3]Department of Pediatrics, University of Illinois College of Medicine, Chicago, IL, United States of America

[4]Faculty of Biology and Biotechnology, University of Science, Vietnam National University, Ho Chi Minh city, Vietnam

Correspondence

Nhung Hai Truong, Laboratory of Stem Cell Research and Application, University of Science, Vietnam National University, Ho Chi Minh city, Vietnam

Faculty of Biology and Biotechnology, University of Science, Vietnam National University, Ho Chi Minh city, Vietnam

Email: thnhung@hcmus.edu.vn

Check for updates

BioMedPress
The Open Access Publisher

ABSTRACT

Introduction: Biliary atresia (BA) is the leading cause of liver fibrosis and failure in neonates with surgical jaundice, leading to poor outcome. Clinical and animal studies showing that granulocyte colony-stimulating factor (GCSF) treatment could improve liver fibrosis and cirrhosis suggest that GCSF may be offered as a low-cost intervention to improve the course of BA. This study aims to test the hypothesis that 10 μg/kg/day x 5 days of GCSF could improve liver function, reduce molecular pro-fibrotic markers and decrease liver fibrosis in a mouse model of bile duct ligation (BDL). **Methods:** Balb/c mice underwent Sham surgery, or BDL for seven days followed by subcutaneous GCSF administration at 10 μg/kg/day for five consecutive days. Twelve days post-operation, blood samples were taken from the facial vein for leukocyte/neutrophil count and for measurement of serum enzymatic activities. The median lobe of the liver was acquired for total RNA and protein extraction. Moreover, the median liver lobe was used for hematoxylin-eosin staining, sirius red staining, and for visualization by immunohistochemistry (IHC). **Results**: Twelve days post-operation, GCSF-treated bile duct-ligated (BDL) mice had a higher survival rate than that of placebo-treated mice (hazard ratio=1.88, p=0.084). The GCSF-treated mice had diminished liver serum transaminase activities (AST: 228.92 ± 222.67 *vs.* 313.46 ± 164.80 IU/L; ALP: 573.24 ± 177.89 IU/L *vs.* 471.75 ± 117.92 IU/L). GCSF treatment also reduced fibrosis with down-regulation of expression of pro-fibrotic markers including TGF-β1 (-2.61-fold mRNA), α-SMA (-2.46-fold mRNA; -1.88-fold protein, p<0.001) and collagen (-3.28-fold mRNA; -1.79-fold collagen deposit, p=0.0055). Moreover, GCSF treatment led to an improvement of histological grade and a reduction of extension of ductular structures caused by cholestasis (-1.77-fold CK7-positive bile ducts, p<0.0001; -2.33-fold CK7 positivity, p<0.0001). **Conclusion:** Administration of GCSF (10 μg/kg/day) for five consecutive days improved the pathological condition of BDL mice. In this study, the positive effect of GCSF could be eventually surpassed due to end-stage liver disease caused from BDL in the mouse model. Further experiments are required to elucidate the effects and mechanisms of GCSF on bile obstruction.

Key words: bile duct ligation, GCSF, Biliary atresia, liver fibrosis

INTRODUCTION

Biliary atresia (BA) is a rare neonatal congenital disease with a prevalence of 1/10,000 to 1/25,000 births and is characterized by obstruction to bile flow from injuries to the bile ducts. It is the most common indication for pediatric liver transplantation. Contributing factors of BA are both congenital and environmental, yet specific causes of the disease remain unknown [1,2]. Untreated BA is fatal, with a median survival of 8 months of age. In BA, fibro-obliterative bile duct injuries cause intra-hepatic and extra-hepatic bile obstruction, persistent liver inflammation, fibrosis, and advanced liver failure [3–5]. The hepatoportoenterostomy (also known as Kasai) procedure is offered to improve bile flow, but the success rate decreases with time and the majority of patients require liver transplantation for long — term survival. The transplantation option is limited in developing countries.

Granulocyte colony-stimulating factor (GCSF) has been used to reduce the risk of infection for innate or acquired neutropenia by enhancing neutrophil production with minimal adverse effects [6–8]. GCSF was exploited as a mobilizing agent of hematopoietic stem cells (HSC s) to increase peripheral blood stem cell harvest efficiency during allogeneic or autologous stem cell transplantation [9,10] for the treatment of many diseases, such as liver disease [11,12]. Moreover, compared to the labor-intensive procedure of harvesting and reinfusing stem cells, GSCF injection alone has been shown to have multiple beneficial effects on liver disease [13,14]. According to systematic reviews, GCSF treatment of patients with advanced liver failure [15,16] and acute-on-chronic liver

failure [17] significantly improved survival or significantly reduced short-term mortality compared to placebo. The *in vivo* mechanisms include the following: GCSF mobilization of HSC homing and differentiating into hepatocytes in CCl4 mice to improve liver functions [18]; increase of neutrophil circulation in the peripheral blood and neutrophil maturation to decrease the risk of infection in patients with end-stage liver disease [13,19]; reduction of CD8 T cells and increase of regulatory T cells (T-regs) [19]; and Kupffer cell activation to reduce inflammation in the injured liver [20]. Furthermore, GCSF promotes endogenous repair mechanisms, increasing the number of proliferating hepatocytes in CCl4 mice [21] and enhancing proliferation of liver progenitor cells (oval cells) [22]. These lines of evidence suggest that GCSF could be used to support the failing liver in BA.

In this study, we performed bile duct ligation (BDL) of Balb/c mice as a model of cholestatic liver disease to test the hypothesis that GCSF improves liver function and decreases fibrosis of intrahepatic biliary diseases, such as BA.

MATERIALS AND METHODS

Mouse strain

The study was approved by our Institutional Ethics Committee (Laboratory of Stem Cell Research and Application, University of Science, Vietnam National University (VNU)-Ho Chi Minh City (HCMC)). Healthy, 8-week old male Balb/c mice from Pasteur Institute in HCMC (Vietnam) were kept in a stable environment of 12 hours light-dark cycle in the microventilation cage system (THREE-SHINE Inc., Korea) with *ad libitum* access to food and water, and were acclimated for 1 week prior to the operation.

Bile duct ligation (BDL) and experiment design

In this study, the BDL procedure was performed as described by Carmen Tag *et al.* [23]. The common bile duct was ligated between sutures and divided with care to avoid injury to the portal vein and the pancreas. Intramuscular (i.m.) administration of 10 mg/kg Ilium xylazil-20 (Troy Laboratories, Australia) was used as a sedative, followed by 7 mg/kg of Zoletil (Virbac, France). Lincomycin (Vemedim, Vietnam) at 20 mg/kg x 2 doses/day was given for 3 days i.m. to prevent post-surgery infections. BDL mice with visible jaundice at 7 days post-operation (d.p.o) were divided into three treatment groups (n=5):

(1) Sham-surgery treated with 200 μl/day of NaCl (0.9% solution);

(2) BDL with Placebo as 200 μl/day of NaCl (0.9% solution); and

(3) BDL + GCSF (10 μg/kg/day; Neupogen® Syringe (Filgrastim) (Roche, Switzerland)).

All treatments were administered subcutaneously (s.c.) starting on d.p.o 8 for 5 consecutive days, and mice were humanely sacrificed the day after the last dose of GCSF (on day 13 post surgery).

Blood sample preparation

Blood samples were taken from the facial vein. Leukocyte and neutrophil counts were calculated by trained and blinded observers using the blood film technique. In brief, a drop of the blood sample was smeared upon a glass slide, air-dried for 3 minutes, fixed in absolute methanol for 5 minutes, and then stained with Giemsa's azure eosin methylene blue solution (Merck Millipore, Germany). Serum aspartate aminotransferase, alkaline phosphatase, and albumin levels were assayed using the GOT (ASAT) IFCC mod. liquiUV kit (HUMAN Diagnostics, Germany), QuantiChrom^{TM} Alkaline Phosphatase Assay Kit (BioAssay Systems, USA), and QuantiChrom^{TM} BCG Albumin Assay Kit (BioAssay Systems, USA), respectively. Data were acquired and analyzed by the DTX 880 Multimode Detector system (Beckman Coulter, USA).

Real-time RT-PCR analysis

Total RNA was extracted from the median lobe of the liver with easy-spin (DNA-free) Total RNA Extraction Kit (iNtRON, Korea). The cDNA was synthesized using SensiFAST^{TM} cDNA Synthesis Kit (Bioline, UK). Real-time RT-PCR analyses were performed using SensiFAST^{TM} SYBR® Hi-ROX Kit (Bioline, UK), and then data were acquired and analyzed on the LightCycler® 480 Instrument II (Roche Life Science, USA) in reference to the Livak's $2^{-\Delta\Delta Ct}$ method [24]. Primers used in this study are shown below:

Immunohistochemistry

For immunohistochemistry and Western blot analysis, the primary antibodies used were anti-cytokeratin 7 (ab181598) and smooth muscle actin-alpha (ab15734) (both from Abcam, MA, USA), β-actin (13E5, Cellsignaling, MA, USA). The secondary antibody was horseradish peroxidase-conjugated secondary goat-anti-rabbit (ab6721, Abcam, MA, USA). Liver tissue used in these analyses was from the median lobe.

The IHC procedure was previously described [25]. In brief, slides were blocked in goat serum blocking

Table 1: Primers used in this study

Gene	Forward (5'-3')	Reverse (5'-3')	ID
TGF β1	TGACGTCACTGGAGTTG-TACGG	GGTTCATGTCATGGATG-GTGC	NM_011577.2
α – SMA	GCATCCACGAAACCACCTA	CACGAGTAACAAATCAAAGC	NM_007392.3
Collagen type I α1	CCTGGACGCCATCAAGGTCTAC	CCAAGTTCCGGTGTGACTCG	NM_007742.4
Gapdh	TCACCATCTTCCAGGAGC	TCACCATCTTCCAGGAGC	NM_001289726.1

buffer (2% Goat serum, 1% BSA, 0.1% Triton X100, 0.05% Tween-20 in phosphate-buffered saline, pH 7.2-7.4, with 0.05 % sodium azide) before incubating with primary α-smooth muscle actin (α-SMA) (1:200) or anti-cytokeratin 7 (CK7) antibody (1:5000). Slides were incubated with peroxidase blocking buffer, *i.e.* 3% hydrogen peroxide (H_2O_2) in PBS, for 10 minutes at RT to block intracellular peroxidase, and then incubated with secondary antibody (1:500) in Tris-buffered saline (TBS) solution with 1% bovine serum albumin (BSA) for 1 h at RT. Immunocomplexes were developed using the ACE kit (Sigma-Aldrich, St Louis, MO). Hematoxylin-Gill III (Merck Millipore, Germany) was used for counterstaining. To quantify the CK7-positive ductal structures around the portal area, 10 random images/slide x 3 slides/mice were captured at x200 magnification. The CK7-positive bile duct densities were calculated as the number of CK7-positive bile ducts divided by tissue surface area.

Western Blot

Liver tissue was instantly frozen in liquid nitrogen and preserved at -80° C until use. Ten mg of tissue was digested and then protein concentration was identified by Pierce BCA Protein Assay Kit (Thermo Fisher Scientific, USA) using DTX 880 Multimode Detector system (Beckman Coulter, USA). Protein samples were subjected to SDS-PAGE on the SE 250 Minivertical Unit (GE Healthcare Life Sciences, USA) at 100 V for 3 h. T he protein bands were transferred into the Immun-Blot® PVDF Membrane (BIO-RAD, Singapore) in the Western blot blotting tank (GE Healthcare Life Sciences, USA) at 100 V for 3 h. The membrane was pre-blocked with TBS (containing 0.1% Tween 20), 5% skimmed milk for 30 minutes before incubation with the appropriate antibodies (primary α-SMA (1:1000) or CK7 (1:5000) or beta-actin (1:6000)) dissolved into TBS (containing 0.1% Tween 20) and 0.5% skimmed milk at 4 o C for 12 h. Signals were developed using Clarity^{TM} Western ECL Kit (BIO-RAD, USA) and visualized by Azure

c300 Chemiluminescent Western Blot Imaging System (LifeGene, Israel). The band intensity was measured by the free software Image Studio^{TM} Lite (LI-COR Biosciences, USA).

Histological analysis

Mouse liver tissue was obtained from the median lobe, fixed in 4% paraformaldehyde (Merck Millipore, Germany), and sectioned from the core of the tissue mass. The tissue was paraffin-embedded and cut into 4 μm slices, with each cross-section approximately 1 mm apart.

Hematoxylin-Eosin staining : Liver slides were stained with Papanicolaou's solution 1a (also called Harris' hematoxylin solution) (Merck Millipore, Germany) and Eosin Y (0.5 %) aqueous solution (Merck Millipore, Germany) according to the protocols afore mentioned.

Picrosirius red staining and relative-quantification of the collagen-positive area: Liver slides were stained with Picrosirius Red Stain Kit (Polysciences, PA, USA) according to the manufacturer's instructions. Collagen accumulation around the portal areas and inside the liver parenchyma (excluding the blood vessels) of the liver lobule (at 10 lobules/slice x 5 slices/mouse) was determined by switching the captured images into the green channel in the RGB stack mode to highlight the red-stained collagen (ImageJ 1.51r software). A trained and blinded observer analyzed the area percentage of positive sites.

Statistical analysis

Data in this study were analyzed and performed by the software GraphPad Prism 6 (GraphPad Inc ., USA). For survival analysis, the Log-rank (Mantel-Cox) test was used. Differences were considered as statistically significant if p-value $\leq$ 0.05. For boxplot comparison, the difference between medians (DBM) and overall visible spreading (OVS) was calculated. The two groups were considered significantly different if DBM/OVS was $\geq$ 50%.

The calculations were as follows: *difference between medians* (DBM)=$|median(1) - median(2)|$; *overall*

visible spread (OVS)=Q3-Q1 in which Q3 is the larger 3rd quartile value and Q1 is the smaller 1st quartile value.

RESULTS

Biliary obstruction diminishes liver function of BDL mice

At 7 days, BDL mice showed jaundice and ruffling (**Figure 1**a), and visible bile duct obstruction with full gallbladder at sacrifice (**Figure 1**b). The serum activity of aspartate transaminase (AST) significantly increased (p=0.0022), with a decline in albumin (ALB) concentration, when compared to those of sham mice (**Figure 1**c) (p=0.03).

GCSF administration increases leukocyte/neutrophil count and reduces the mortality rate of BDL mice

After 5 days of GCSF, consistent with GCSF 's effect on mobilizing bone marrow cells, the total serum leukocyte count in GCSF-treated mice reached $32.72\pm13.49 \times 10^6$ cells/ml (n=5), while that of the placebo was $10.46 \pm 4.99 \times 10^6$ cells/ml (n=4) (p<0.05) (**Figure 2**a). The neutrophil count in GCSF-treated mice was $27.83\pm14.41\times10^6$ cells/ml (n=5), compared to $6.48\pm2.87 \times 10^6$ cells/ml (n=4) in the placebo group (p<0.05) (**Figure 2**b). The corresponding median survival of GCSF-treated BDL mice (n=10 for each group) was 13.0 days, as compared to 10.5 days for placebo-BDL mice, with a hazard ratio (log -rank) of 1.88 (**Figure 2**c) (p= 0.08 nearing statistical significance).

GCSF reduces elevation of serum transaminases in BDL mice

There was a decrease in serum aspartate aminotransferase (AST) concentration in BDL mice treated with GCSF (median serum AST: 116.33 IU/L), compared to those BDL mice treated with placebo (median serum AST: 297.76 IU/L) (DBM/OVS=51.23%) (**Figure 3**a). This was not seen with serum ALP or albumin values (**Figure 3**b, c). Though positive results were seen, these indicators did not fully reflect the disease condition in treated mice and were not significant different (**Figure 3,** p>0.05); this was expected as bile duct obstruction was fixed[26].

GCSF administration reduces the expression of pro-fibrotic markers in BDL mice

Down-regulation of mRNA levels of pro-fibrotic genes in GCSF-treated BDL mice were observed, with notable decrease in the levels of *TGF-β* mRNA (2.61 fold-change, DBM/OVS=85.99%), α *-SMA* (2.46 fold-change, DBM/OVS=22.83%), and *col1a1* (3.28 fold-change, DBM/OVS=69.41%) (**Figure 4**). A parallel reduction in the amount of collagen deposit by 1.79-fold (p=0.006) was seen around and across portal areas (bridging fibrosis) of the GCSF treated BDL mice compared to placebo (**Figure 5**).

Similarly, consistent with the down regulation of α*-SMA* expression, Western blot data showed a 10.46 ± 0.36 and 5.56 ± 0.81 fold-change for BDL and GCSF-BDL groups, respectively, compared to that for sham mice (p<0.0001) (**Figure 6**). Immunostaining confirmed a decreased periportal α-SMA expression in GCSF-treated liver of BDL mice (**Figure 7**).
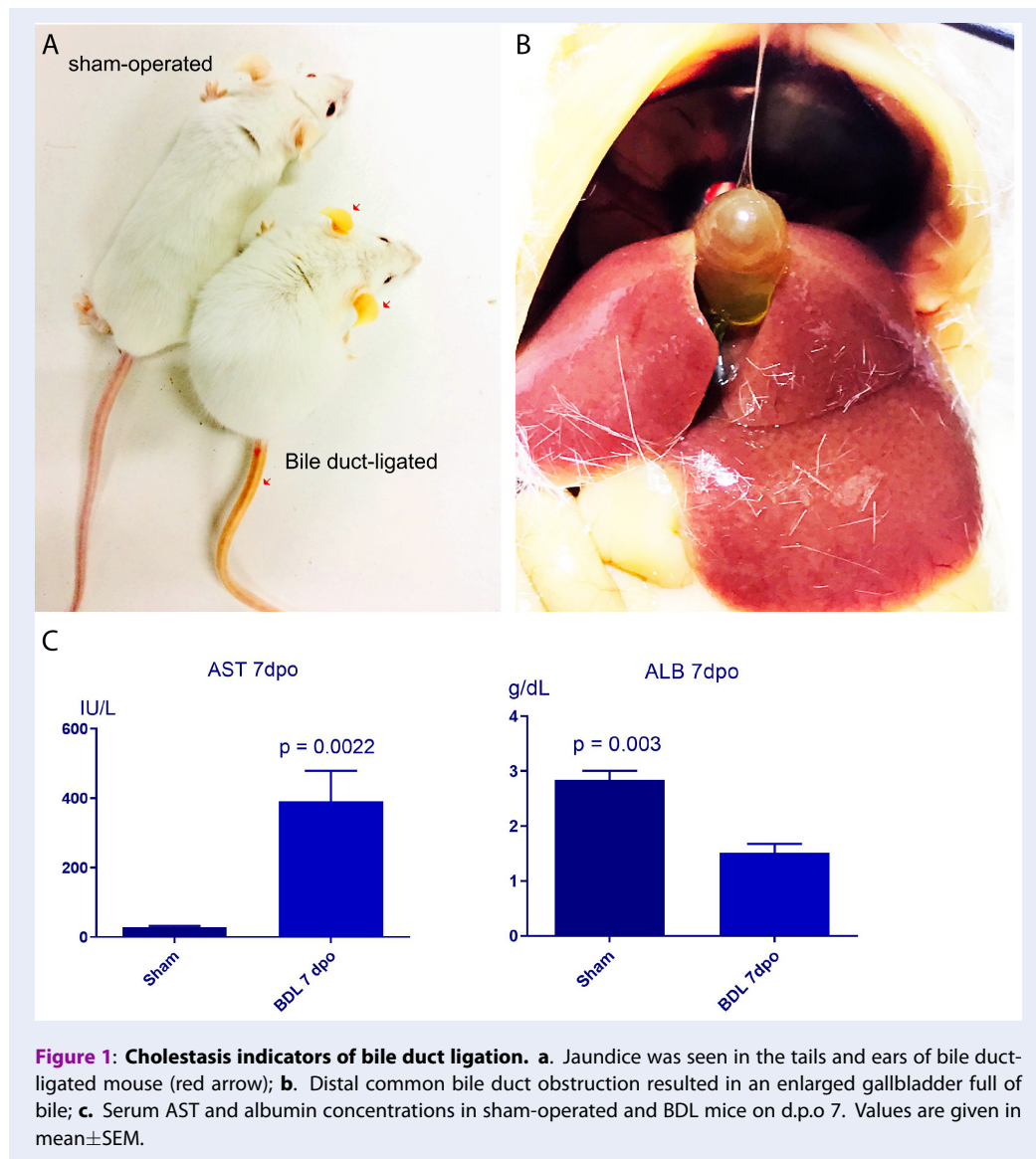
GCSF administration improves histology injury and reduces ductal reaction

There was significant improvement in the liver histology of GCSF-treated BDL mice compared to that of BDL mice, with fewer infarction zones (**Figure 8**) from BDL bile necrosis. Moreover, as previously mentioned, there was less bridging fibrosis (**Figure 5**d: -1.79-fold change, p=0.006) around the expansion areas of ductal structures (**Figure 9**d: -1.77-fold change, p<0.0001) in the GCSF-treated BDL mice.

In compensation to hepatic injury, bile duct progenitor cells proliferate to expand the ductal structures[27]. This was seen in the portal areas of BDL liver with a high number of cytokeratin-7 (CK-7) positive newly formed ductal structures (**Figure 9**b) (41.12 ± 1.1 bile ducts/mm^2). GCSF treatment reduced the number of CK7 positive bile ducts (23.2 ± 2.75 bile ducts/mm^2) (1.77-fold change, p<0.0001), as well as decreased whole liver CK7 protein levels (2.33-fold reduction, p<0.0001) (**Figure 10**).

DISCUSSION

In this study, bile duct ligation (BDL) leads to obstructive jaundice, hepatomegaly, increased hepatic transaminase levels, and decreased liver functions (such as albumin levels). Since Balb/c mice are more vulnerable to hepatic fibrosis[28] and liver injury, with a high mortality by 14 days of surgery compared to other strains of mice, this study was limited to a 12-day course after mice exhibited liver injury by the 7th day and after completion of the 5 doses of GCSF treatment. In this study, administration of 5 doses of 10 μg/kg/day to BDL Balb/c mice increased the leukocyte and neutrophil counts in peripheral blood of these mice, compared to that for placebo-treated mice (p<0.05). Our results showed that administration of GCSF improved the mortality in GCSF-treated BDL mice compared to the placebo (hazard ratio=1.88)[27]. In this study, GCSF-treated BDL

Figure 1: **Cholestasis indicators of bile duct ligation. a**. Jaundice was seen in the tails and ears of bile duct-ligated mouse (red arrow); **b**. Distal common bile duct obstruction resulted in an enlarged gallbladder full of bile; **c**. Serum AST and albumin concentrations in sham-operated and BDL mice on d.p.o 7. Values are given in mean±SEM.

mice had low AST activities compared to placebo-treated BDL mice, suggesting a less injured liver [21,27]. Furthermore, GCSF diminished the liver fibrosis via down regulation of pro-fibrotic genes, such as *TGF-β1, α-SMA,* and *col1a1.* This was consistent with reduction of α-SMA protein level (confirmed by IHC and Western blot) and collagen deposit (confirmed by Sirius red staining) [21].

This model of liver injury adds to the list of other experimental models of liver injury, including partial hepatectomy in rats [22], radiation [29], acute failure from thioacetamide (TAA) [30], D-galactosamine [31], CCl$_4$ [32] and NAFLD [33] publications show the beneficial effects of GCSF on the attenuation of hepatic injury (adjust references).   Underlying the attenuated hepatic in-

jury are various phenomena, including the reduction of the inflammatory response, the promotion of endogenous repair [21], increase in hepatocyte proliferation [34,35] with increased PI3K/Akt pathways [33], development of oval cell proliferation [22], and reduction in the apoptotic drive [33].

During liver injury, a correlation between ductular reaction and fibrogenesis, presumably from the extracellular synthesis of the newly forming bile ducts, have been reported [36-38].   Inhibition of the ductular response reduced liver fibrosis in MDR2 $^{-/-}$ mice [39]. In this study, G-CSF significantly reduced cytokeratin-7 (CK7) expression and the number of CK7-positive ductal structures in BDL mice, providing a novel effect of GCSF on improving liver injury by diminishing
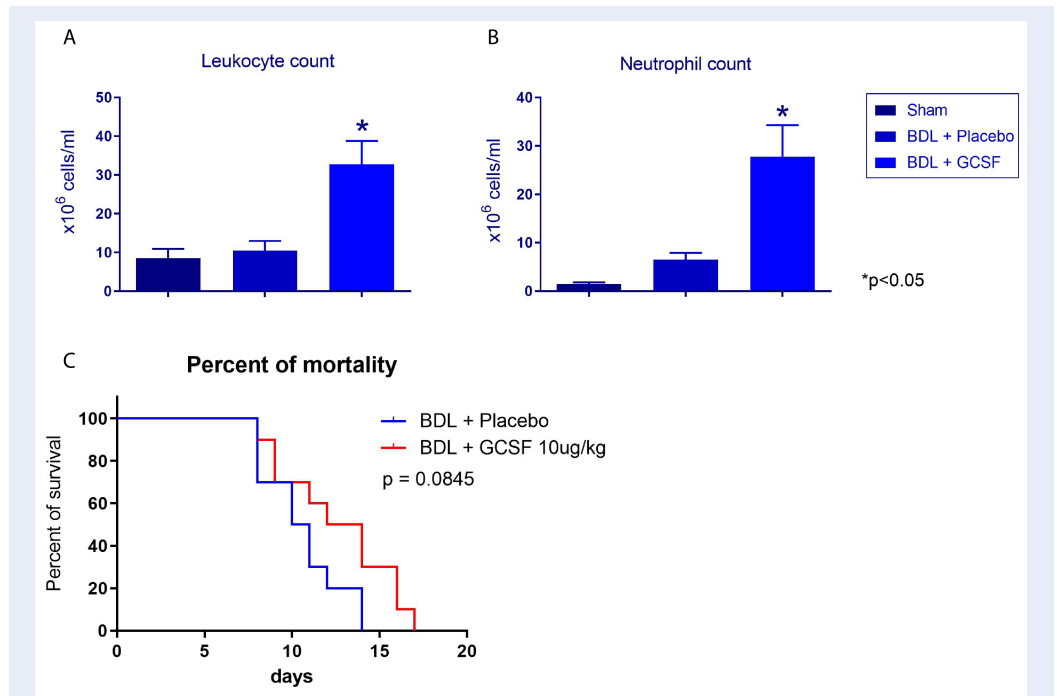
Figure 2: **Leukocyte/neutrophil count (a) and (b) with values depicted as the mean±SEM and (c) Kaplan meier survival curve for the 3 treatment groups.**
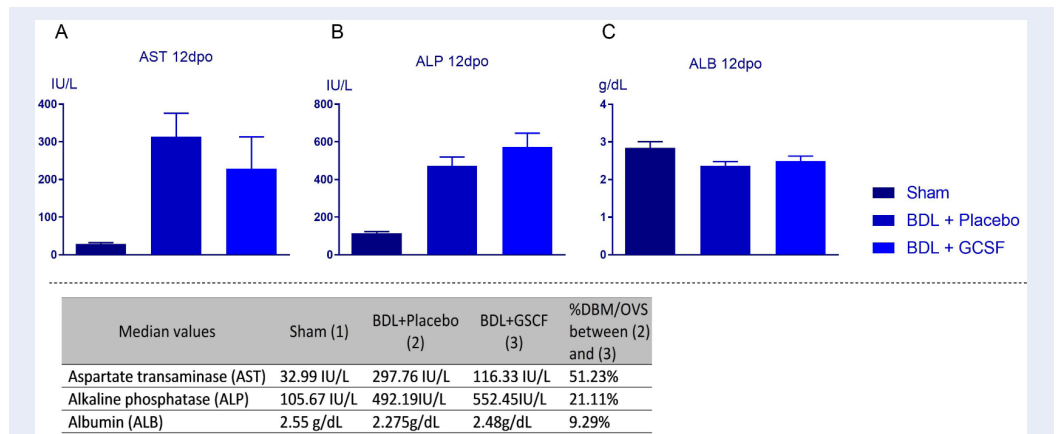

Median values	Sham (1)	BDL+Placebo (2)	BDL+GSCF (3)	%DBM/OVS between (2) and (3)
Aspartate transaminase (AST)	32.99 IU/L	297.76 IU/L	116.33 IU/L	51.23%
Alkaline phosphatase (ALP)	105.67 IU/L	492.19IU/L	552.45IU/L	21.11%
Albumin (ALB)	2.55 g/dL	2.275g/dL	2.48g/dL	9.29%

Figure 3: **Liver biochemical indexes**. The line inside each box illustrates the median value of each group of treatment in Sham and BDL mice.

the ductular reaction. Future studies into the mechanism of GCSF protective effects in liver injury should target the relationship between GCSF and the ductular response. It is worth noting that the histopathological features of biliary atresia include portal fibrosis and inflammation, but also ductular proliferation[39]. Therefore, these evidence provides a rationale for the use of GCSF as an intervention for BA.

CONCLUSION

In this experimental model of intermediate-term liver damage by obstructive BDL injury, post-injury treatment with GCSF improved the hepatic outcome of bile duct-ligated mice, notably a reduction in hepatic fibrosis and its association with down regulation of the ductular reaction. GCSF may be useful as a treatment for liver fibrosis in BA disease.
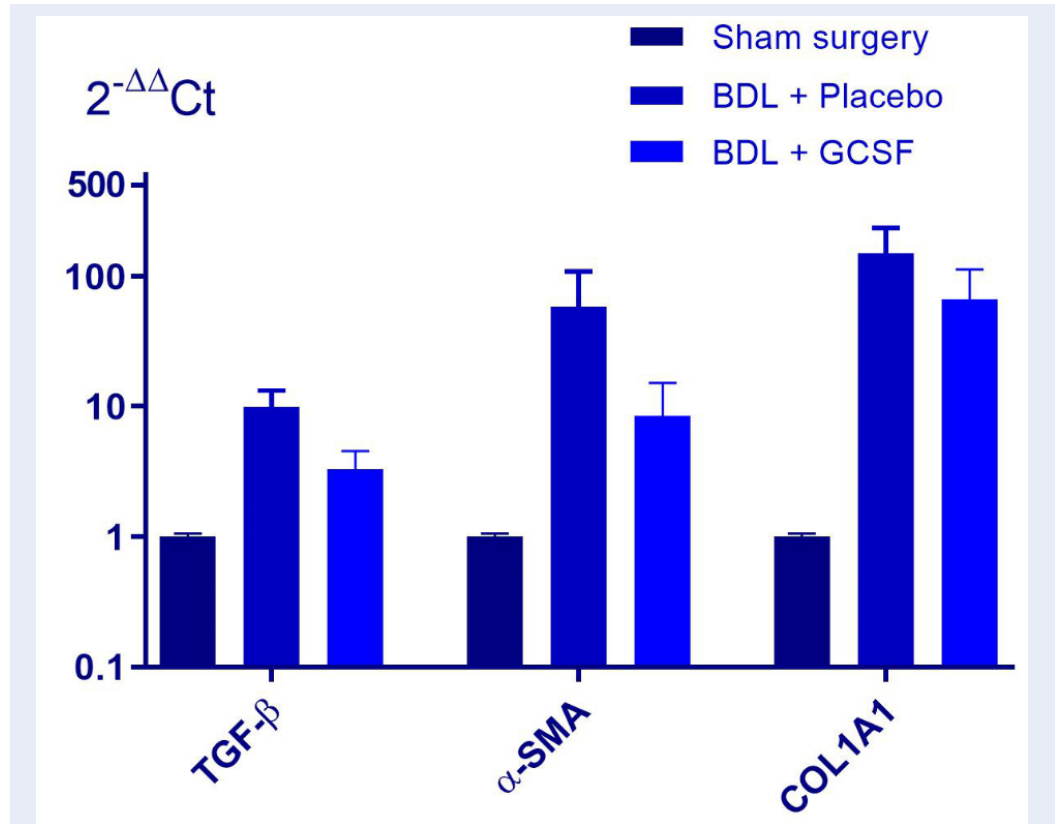
Figure 4: **mRNA expression in all treatment groups**. Graph showing the median value of 2^{-DDCT} *tgfβ*, *α-SMA* and *col1a1* gene expression for each treatment group normalized to that of sham.
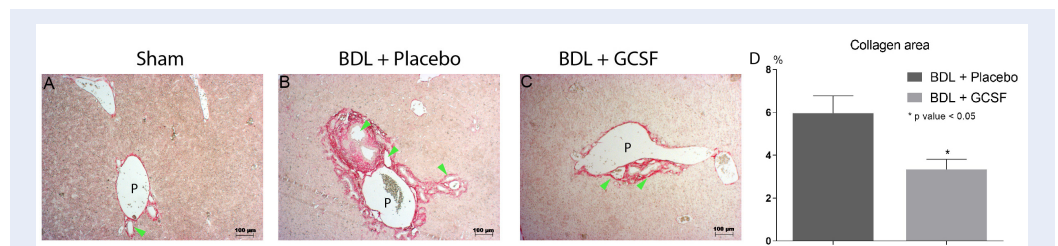

Figure 5: **Periportal Collagen deposit in operated mice**. Collagen-positive Sirius red stained zones around the vasculature of the portal vein and bile duct in (**a**) sham operated, (**b**) BDL and (**c**) GCSF-BDL liver showing denser periductal collagenous structures and increases of newly formed bile ducts in the portal tract in BDL liver (green arrows) with fewer periportal collagen-positive accumulation in GCSF-BDL liver; and graph showing the quantitative analyses in the Sirius red collagen deposits.
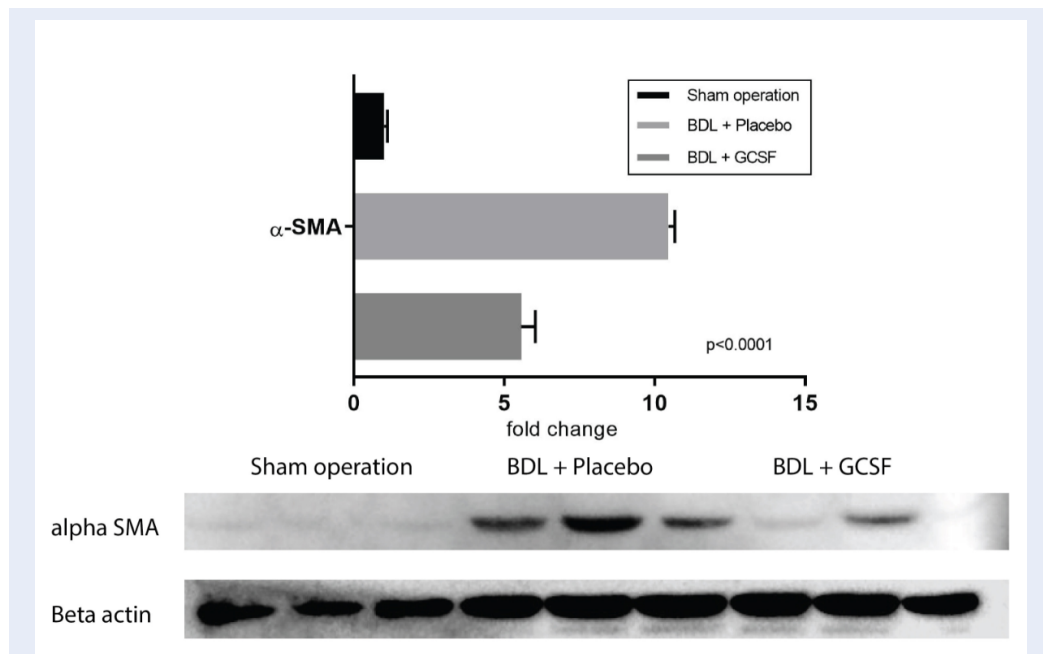
Figure 6: **Western blot analysis of α-SMA expression in operated mice**. The intensity of protein bands in BDL groups were quantitated.
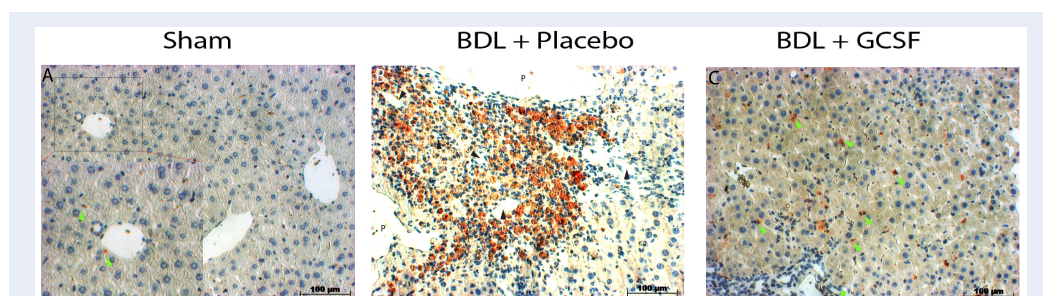
Figure 7: **Immunostaining for aSMA in the liver:** In sham mice, α-SMA is expressed in both quiescent and activated hepatic stellate cells, residing among larger hepatocytes (**a**, light green arrows); with strong expression of α-SMA in the placebo-BDL mice around the portal area (black arrows) (**b**) and significant reduction in α-SMA positivity in GCSF-BDL mice (**c**) P standsfor the portal vein.

ABBREVIATIONS

ALB: Albumin

ALP: Alkaline photphatase

AST: Aspartate transaminase

BA: Biliary Atresia

BDL: Bile duct ligation

CK7: Cytokeratin-7

GCSF: Granulocyte colony stimulating factor

HSC: Hematopoietic stem cell

IHC: Immunohistochemistry

MELD: Model for End-stage Liver Disease

NAFOSTED: National Foundation for Science and Technology Development

α**SMA**: alpha Smooth Muscle Actin

TGFβ: Transforming Growth Factor beta

AUTHOR CONTRIBUTION

Huy Quang Do conducted the experiments and composed the manuscript. Trinh Van Le, Minh Thanh Dang, Tien-Trieu Pham-Le and Luan Van Chan carried out the experiments and analyzed the liver function, gene-expression and histology. Khon Chan Huynh performed and analyzed the protein expression. Ai-Xuan Le Holterman is senior researcher, ad-
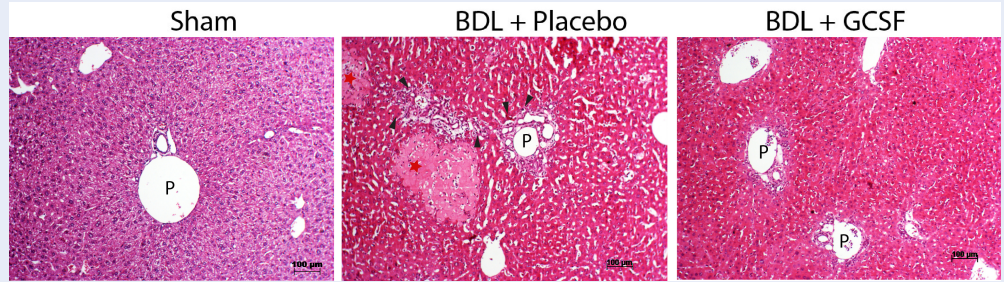
Figure 8: **Hematoxylin and Eosin staining of portal areas**. Cross section of a portal zone from (**a**) sham operated mice showing the portal vein and the associated bile duct(s), and a homogeneous, regular parenchymal surface; (**b**) bileduct-ligated mouse showing abnormal proliferation of ductal structures (black arrows) and bridging fibrosis between the portal tracts. Red stars indicate areas of infarction; and (**c**) the portal areas of the GCSF-treated mice. (P): Portal veins
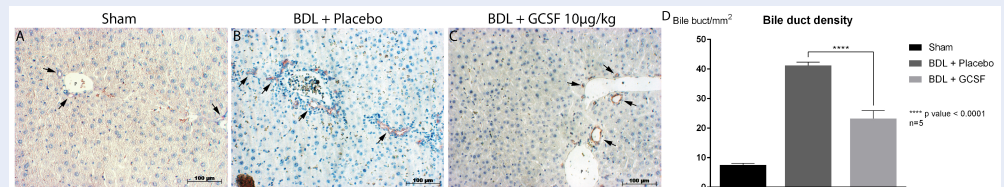

Figure 9: **Expansion of cytokeratin-7 (CK-7) positive cells following BDL is diminished with GCSF treatment.** Liver micrographs showing CK7 positive cells as indicated by the black arrows in (**a**) normal mice showing a small population of CK-7 positive progenitor cells; (**b**) placebo BDL mice with expanded CK-7 positive ductal structures (**c**) GCSF-BDL mice, with fewer CK-7 positive bile ducts compared to BDL mice; (**d**) bile duct density as measured by the average number of ducts/mm^2. P stands for the portal vein.
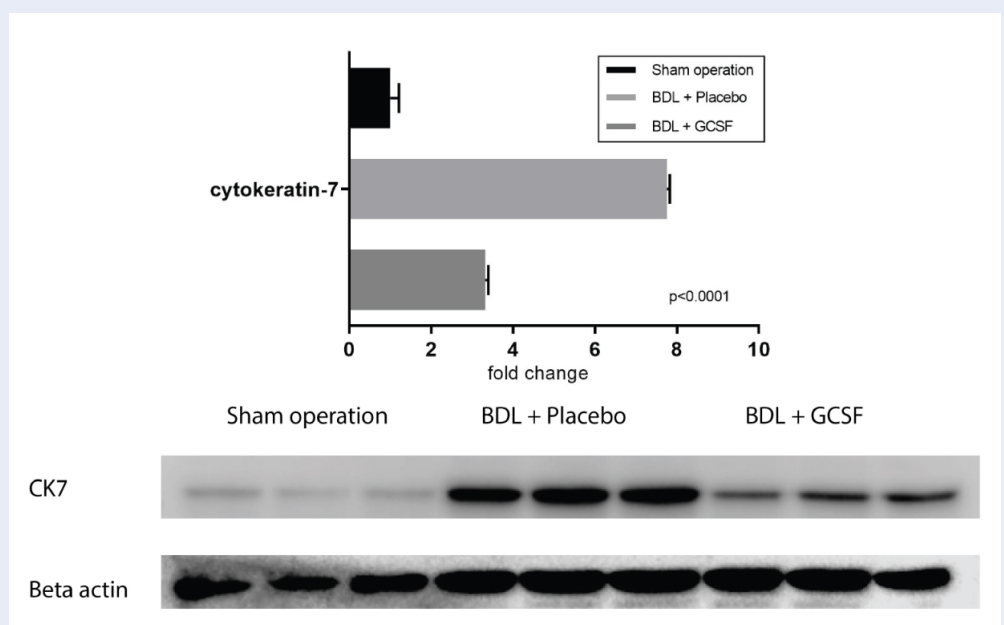
Figure 10: **Western blot analysis ofcytokeratin-7 expression in operated mice.** The intensity of protein bands in BDL groups were quantitated showing a 7.77±0.13 and 3.32±0.13fold-change for BDL and GCSF-BDL relative to sham mice.

vices on the design of experimental models and on data analyses and revise the manuscript. Nhung Hai Truong made substantial contributions to the ideas, experiment design , interpretation of data, and submission.

COMPETING INTERESTS

The authors declare that they have no competing interests.

ACKNOWLEDGEMENT

REFERENCES

1. Lakshminarayanan B, Davenport M. Biliary atresia: A comprehensive review. J Autoimmun. 2016;73:1–9. PMID: 27346637. Available from: 10.1016/j.jaut.2016.06.005.
2. Nakamura K, Tanoue A. Etiology of biliary atresia as a developmental anomaly: recent advances. J Hepatobiliary Pancreat Sci. 2013;20(5):459–64. PMID: 23567964. Available from: 10.1007/s00534-013-0604-4.
3. Bates MD, Bucuvalas JC, Alonso MH, Ryckman FC. Biliary atresia: pathogenesis and treatment. Semin Liver Dis. 1998;18(3):281–93. PMID: 9773428. Available from: 10.1055/s-2007-1007164.
4. Hays DM, Snyder WH. Life-span in untreated biliary atresia. Surgery. 1963;54(2):373–5. PMID: 14048039.
5. Adelman S. Prognosis of uncorrected biliary atresia: an update. J Pediatr Surg. 1978;13(4):389–91. PMID: 682088. Available from: 10.1016/S0022-3468(78)80462-X.
6. Panopoulos AD, Watowich SS. Granulocyte colony-stimulating factor: molecular mechanisms of action during steady state and 'emergency' hematopoiesis. Cytokine. 2008;42(3):277–88. PMID: 18400509. Available from: 10.1016/j.cyto.2008.03.002.
7. Carr R, Modi N, Dore C. G-CSF and GM-CSF for treating or preventing neonatal infections. The Cochrane database of systematic reviews. 2003;2003(3):Cd003066.
8. Kraj L, Krawczyk-Lipiec J, Górniewska J, Orlik G. Efficacy and safety of biosimilar filgrastim in primary and secondary prevention of febrile neutropenia. Biomed Rep. 2017;7(2):143–7. PMID: 28804626. Available from: 10.3892/br.2017.938.
9. Bendall LJ, Bradstock KF. G-CSF: from granulopoietic stimulant to bone marrow stem cell mobilizing agent. Cytokine Growth Factor Rev. 2014;25(4):355–67. PMID: 25131807. Available from: 10.1016/j.cytogfr.2014.07.011.
10. Publicover A, Richardson DS, Davies A, Hill KS, Hurlock C, Hutchins D, et al. Use of a biosimilar granulocyte colony-stimulating factor for peripheral blood stem cell mobilization: an analysis of mobilization and engraftment. Br J Haematol. 2013;162(1):107–11. PMID: 23614650. Available from: 10.1111/bjh.12345.
11. Salama H, Zekri AR, Medhat E, Alim SAA, Ahmed OS, Bahnassy AA, et al. Peripheral vein infusion of autologous mesenchymal stem cells in Egyptian HCV-positive patients with end-stage liver disease. Stem Cell Res Ther. 2014;5(3):70. PMID: 24886681. Available from: 10.1186/scrt459.
12. Terai S, Ishikawa T, Omori K, Aoyama K, Marumoto Y, Urata Y, et al. Improved liver function in patients with liver cirrhosis after autologous bone marrow cell infusion therapy. Stem Cells. 2006;24(10):2292–8. PMID: 16778155. Available from: 10.1634/stemcells.2005-0542.
13. Duan XZ, Liu FF, Tong JJ, Yang HZ, Chen J, Liu XY, et al. Granulocyte-colony stimulating factor therapy improves survival in patients with hepatitis B virus-associated acute-on-chronic liver failure. World J Gastroenterol. 2013;19(7):1104–10. PMID: 23467275. Available from: 10.3748/wjg.v19.i7.1104.
14. Duan XZ, Liu FF, Tong JJ, Yang HZ, Chen J, Liu XY, et al. Granulocyte-colony stimulating factor therapy improves survival in patients with hepatitis B virus-associated acute-on-chronic liver failure. World J Gastroenterol. 2013;19(7):1104–10. PMID: 23467275. Available from: 10.3748/wjg.v19.i7.1104.
15. Yang Q, Yang Y, Shi Y, Lv F, He J, Chen Z. Effects of Granulocyte Colony-Stimulating Factor on Patients with Liver Failure: a Meta-Analysis. J Clin Transl Hepatol. 2016;4(2):90–6. PMID: 27350939.
16. Kumar A, Sharma P, Arora A. Granulocyte colony-stimulating factor for advanced liver disease: a meta-analysis. J Hepatol. 2017;66(1):132. Available from: 10.1016/S0168-8278(17)30533-0.
17. Chavez-Tapia NC, Mendiola-Pastrana I, Ornelas-Arroyo VJ, Noreña-Herrera C, Vidaña-Perez D, Delgado-Sanchez G, et al. Granulocyte-colony stimulating factor for acute-on-chronic liver failure: systematic review and meta-analysis. Ann Hepatol. 2015;14(5):631–41. PMID: 26256891. Available from: 10.1016/S1665-2681(19)30757-4.
18. Tsolaki E, Athanasiou E, Gounari E, Zogas N, Siotou E, Yiangou M, et al. Hematopoietic stem cells and liver regeneration: differentially acting hematopoietic stem cell mobilization agents reverse induced chronic liver injury. Blood Cells Mol Dis. 2014;53(3):124–32. PMID: 24923531. Available from: 10.1016/j.bcmd.2014.05.003.
19. Garg V, Garg H, Khan A, Trehanpati N, Kumar A, Sharma BC, et al. Granulocyte colony-stimulating factor mobilizes CD34(+) cells and improves survival of patients with acute-on-chronic liver failure. Gastroenterology. 2012;142(3). PMID: 22119930. Available from: 10.1053/j.gastro.2011.11.027.
20. Busch CJ, Wanner GA, Menger MD, Vollmar B. Granulocyte colony-stimulating factor (G-CSF) reduces not only gram-negative but also gram-positive infection-associated proinflammatory cytokine release by interaction between Kupffer cells and leukocytes. Inflammation research : official journal of the European Histamine Research Society. 2004;53(5):205–10.
21. Yannaki E, Athanasiou E, Xagorari A, Constantinou V, Batsis I, Kaloyannidis P, et al. G-CSF-primed hematopoietic stem cells or G-CSF per se accelerate recovery and improve survival after liver injury, predominantly by promoting endogenous repair programs. Exp Hematol. 2005;33(1):108–19. PMID: 15661404. Available from: 10.1016/j.exphem.2004.09.005.
22. Piscaglia AC, Shupe TD, Oh SH, Gasbarrini A, Petersen BE. Granulocyte-colony stimulating factor promotes liver repair and induces oval cell migration and proliferation in rats. Gastroenterology. 2007;133(2):619–31. PMID: 17681181. Available from: 10.1053/j.gastro.2007.05.018.
23. Tag CG, Sauer-Lehnen S, Weiskirchen S, Borkham-Kamphorst E, Tolba H, et al. Bile Duct Ligation in Mice: Induction of Inflammatory Liver Injury and Fibrosis by Obstructive Cholestasis. JoVE (Journal of Visualized Experiments). 2015;96:e52438.
24. Livak KJ, Schmittgen TD. Analysis of relative gene expression data using real-time quantitative PCR and the 2(-ΔΔC(T)) Method. Methods. 2001;25(4):402–8. PMID: 11846609. Available from: 10.1006/meth.2001.1262.
25. Truong NH, Nguyen NH, Le TV, Vu NB, Huynh N, Nguyen TV, et al. Comparison of the Treatment Efficiency of Bone Marrow-Derived Mesenchymal Stem Cell Transplantation via Tail and Portal Veins in CCl4-Induced Mouse Liver Fibrosis. Stem Cells

Int. 2016;2016:5720413. PMID: 26839564. Available from: 10.1155/2016/5720413.

26. Abshagen K, König M, Hoppe A, Müller I, Ebert M, Weng H, et al. Pathobiochemical signatures of cholestatic liver disease in bile duct ligated mice. BMC Syst Biol. 2015;9(1):83. PMID: 26589287. Available from: 10.1186/s12918-015-0229-0.

27. Strazzabosco M, Fabris L. Development of the bile ducts: essentials for the clinical hepatologist. J Hepatol. 2012;56(5):1159–70. PMID: 22245898. Available from: 10.1016/j.jhep.2011.09.022.

28. Walkin L, Herrick SE, Summers A, Brenchley PE, Hoff CM, Korstanje R, et al. The role of mouse strain differences in the susceptibility to fibrosis: a systematic review. Fibrogenesis Tissue Repair. 2013;6(1):18. PMID: 24294831. Available from: 10.1186/1755-1536-6-18.

29. Zhang L, Kang W, Lei Y, Han Q, Zhang G, Lv Y, et al. Granulocyte colony-stimulating factor treatment ameliorates liver injury and improves survival in rats with D-galactosamine-induced acute liver failure. Toxicol Lett. 2011;204(1):92–9. PMID: 21550386. Available from: 10.1016/j.toxlet.2011.04.016.

30. Li N, Zhang L, Li H, Fang B. Human CD34+ cells mobilized by granulocyte colony-stimulating factor ameliorate radiation-induced liver damage in mice. Stem Cell Res Ther. 2010;1(3):22. PMID: 20633298. Available from: 10.1186/scrt22.

31. Esmaili M, Qujeq D, Yoonesi AA, Feizi F, Ranaee M. Effects of associated SCF and G-CSF on liver injury two weeks after liver damage: A model induced by thioacetamide administration. Mol Biol Res Commun. 2014;3(2):141–7. PMID: 30805380.

32. Zhang L, Kang W, Lei Y, Han Q, Zhang G, Lv Y, et al. Granulocyte colony-stimulating factor treatment ameliorates liver injury and improves survival in rats with D-galactosamine-induced acute liver failure. Toxicol Lett. 2011;204(1):92–9. PMID: 21550386. Available from: 10.1016/j.toxlet.2011.04.016.

33. Qujeq D, Abassi R, Faeizi F, Parsian H, Faraji AS, Taheri H, et al. Effect of granulocyte colony-stimulating factor administration on tissue regeneration due to carbon tetrachloride-induced liver damage in experimental model. Toxicol Ind Health. 2013;29(6):498–503. PMID: 22446100. Available from: 10.1177/0748233712440136.

34. Nam HH, Jun DW, Jang K, Saeed WK, Lee JS, Kang HT, et al. Granulocyte colony stimulating factor treatment in non-alcoholic fatty liver disease: beyond marrow cell mobilization. Oncotarget. 2017;8(58):97965–76. PMID: 29228666. Available from: 10.18632/oncotarget.18967.

35. Kimura M, Yamada T, Iwata H, Sekino T, Shirahashi K, Yoshida N, et al. Preoperative granulocyte-colony stimulating factor (G-CSF) treatment improves congested liver regeneration. J Surg Res. 2010;158(1):132–7. PMID: 19500798. Available from: 10.1016/j.jss.2008.09.002.

36. Rókusz A, Veres D, Szücs A, Bugyik E, Mózes M, Paku S, et al. Links Between Hepatic Fibrosis, Ductular Reaction, and Progenitor Cell Expansion. Gastroenterology. 2017;146(2):349–56. Available from: 10.1371/journal.pone.0176518.

37. Williams MJ, Clouston AD, Forbes SJ. Links between hepatic fibrosis, ductular reaction, and progenitor cell expansion. Gastroenterology. 2014;146(2):349–56. PMID: 24315991. Available from: 10.1053/j.gastro.2013.11.034.

38. Sato K, Marzioni M, Meng F, Francis H, Glaser S, Alpini G. Ductular Reaction in Liver Diseases: Pathological Mechanisms and Translational Significances. Hepatology. 2019;69(1):420–30. PMID: 30070383. Available from: 10.1002/hep.30150.

39. McDaniel K, Wu N, Zhou T, Huang L, Sato K, Venter J, et al. Key Histopathologic Features of Liver Biopsies That Distinguish Biliary Atresia From Other Causes of Infantile Cholestasis and Their Correlation With Outcome: A Multicenter Study. The American journal of surgical pathology. 2016;40(12):1601–15. Available from: 10.1002/hep.30542.